

# GD analysis of arbitrary terminated PD with an unequal power-dividing ratio

ISSN 1751-8725  
Received on 28th November 2018  
Revised 24th January 2019  
Accepted on 12th February 2019  
E-First on 13th March 2019  
doi: 10.1049/iet-map.2018.6116  
www.ietdl.org

Girdhari Chaudhary<sup>1</sup>, Yongchae Jeong<sup>1</sup> ✉

<sup>1</sup>Division of Electronics and Information Engineering, Chonbuk National University, Jeonju, Republic of Korea

✉ E-mail: ycjeong@jbnu.ac.kr

**Abstract:** This study presents the group delay (GD) analysis of an arbitrary terminated unequal power-dividing ratio of a power divider (PD) combined with a negative group delay (NGD) circuit. The proposed circuit can provide an arbitrary prescribed positive group delay (PGD) between ports 2 and 1, whereas it can provide NGD between ports 3 and 1. From analytical analysis, it is found that the magnitude and GD of the PGD path depend only on the power-division ratio, whereas the magnitude and GD of the NGD path depend on the power-division ratio as well as the on NGD circuit. For an experimental verification, the arbitrary terminated unequal PD was designed, fabricated, and measured at the centre frequency of 2.14 GHz. The measurement results are in good agreement with the simulation and predicted theoretical results. For the NGD bandwidth and magnitude flatness enhancement, coupled-line NGD circuits with slightly different centre frequencies connected in parallel were designed and fabricated providing wider bandwidth than the single stage and showed a practical applicability.

## 1 Introduction

In microwave circuits and systems, power dividers (PDs) have been widely adopted as basic building components in various applications. Over the past few decades, PDs have been extensively studied including the unequal and tunable power-division ratio, circuit miniaturisation, and multi-band operation [1–8]. Even though group delay (GD) matching between different paths is essential in various circuits and systems, such as linear series-fed antenna arrays, the investigation of GD characteristics has seldom been carried out. For these circuits and systems, a PD with a negative group delay (NGD) characteristics will be beneficial in order to compensate a positive group delay (PGD).

Various approaches have been applied to the design of two-port active/passive microwave NGD circuits using *RLC* resonators [9–16]. These circuits have been applied in various practical applications in communication systems [9–12]. Since the conventional NGD circuits have a termination impedance of 50 Ω, the extra matching networks are required while integrating with non-50 Ω termination circuits such as arbitrary terminated PDs, which increases circuit size and additional PGDs.

NGD circuits have also been applied to design feed networks for minimising the beam-squint problems of the antenna arrays [17]. However, the conventional feed networks of antenna arrays

designed using NGD circuits suffer from high insertion loss and small fractional bandwidths (FBWs). Also, the NGD circuits and PDs are designed independently in previous works, which require an additional interfacing matching networks to integrate the conventional NGD circuit with arbitrary terminated PD. Therefore, the research that can demonstrate the co-design and GD analysis of arbitrary termination impedance PD and NGD circuit would be promising for the squint free series-fed antenna arrays.

Recently, the NGD PD is presented in [18–20], which suffer from narrow bandwidth and limited to equal power-division ratio and 50 Ω termination impedances. Some efforts have been made to design an arbitrary terminated unequal coupler with PGD and NGD characteristics [21–23]. However, these works suffer from large insertion loss.

In this paper, the GD analysis of the arbitrary termination impedance unequal PD is investigated. In this work, one of two paths in arbitrary terminated PD is replaced with an arbitrary terminated NGD circuit; therefore, it does not require any additional interface matching networks. From theoretical analysis, it is found that the proposed circuit can provide the PGD through input port and one of output port, whereas it can provide NGD through input and another output port. Moreover, the proposed circuit can also provide zero GD and constant phase over large bandwidth by using circuit parameters properly. Therefore, the proposed circuit can be utilised as a feeding network in linear series-fed antenna arrays for a low-squinting beam-forming network.

## 2 Theory and design equations

Fig. 1 shows the proposed structure of unequal PD with arbitrary termination impedances of  $Z_a$ ,  $Z_b$ , and  $Z_c$ . The proposed structure consists of a  $1:k_1^2$  Wilkinson power divider (WPD) and an arbitrary terminated low-signal attenuation (SA) coupled-line NGD circuit. In the proposed structure, the NGD circuit is connected between input port 1 and output port 3 of the WPD. The electrical lengths of transmission lines are  $\lambda/4$  at the designed centre frequency ( $f_0$ ). Similarly, arbitrary terminated low SA NGD circuit consists of branch line where the direct and through ports are terminated with a resistor-connected short-circuited coupled line with an open-circuited isolation port [16]. Since NGD exists near an absorption line or SA condition, where ‘anomalous’ wave propagation effects can occur [10, 18, 19], it is possible to generate

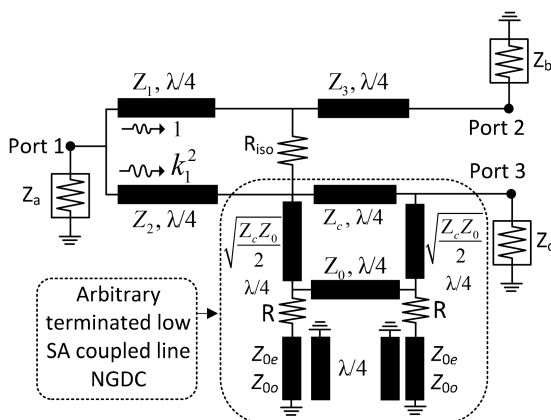


**Fig. 1** Proposed structure of an arbitrary terminated unequal power divider with positive and negative group delays

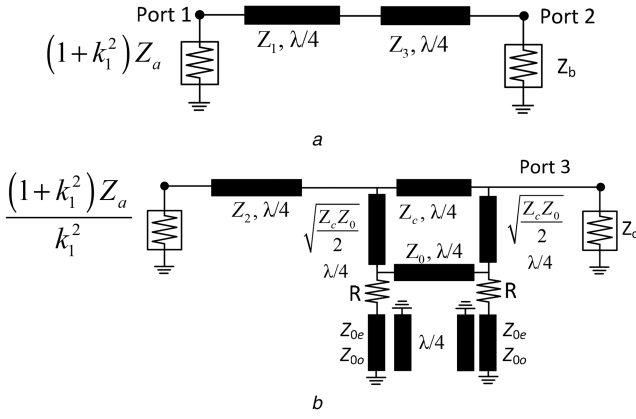


**Fig. 2** Modified even-mode equivalent circuit of the proposed arbitrary terminated unequal power divider  
(a) Between ports 2 and 1 and, (b) Between ports 3 and 1

NGD through SA condition in transmission paths 3 and 1 of the proposed PD because of the resistor-terminated short-circuited coupled line.

Since the proposed structure is not symmetrical, modified even- and odd-mode analyses can be applied to find the  $S$ -parameters and GDs associated with different transmission paths [6, 24].

Using the modified even-mode equivalent circuit shown in Fig. 2a, the even-mode  $S$ -parameters between ports 2 and 1 can be derived as follows:

$$S_{11e}^{21} = \frac{A_e^{21}Z_b + B_e^{21} - C_e^{21}(1+k_1^2)Z_aZ_b - D_e^{21}(1+k_1^2)Z_a}{A_e^{21}Z_b + B_e^{21} + C_e^{21}(1+k_1^2)Z_aZ_b + D_e^{21}(1+k_1^2)Z_a} \quad (1a)$$

$$S_{21e}^{21} = \frac{2\sqrt{(1+k_1^2)Z_aZ_b}}{A_e^{21}Z_b + B_e^{21} + C_e^{21}(1+k_1^2)Z_aZ_b + D_e^{21}(1+k_1^2)Z_a}, \quad (1b)$$

where

$$A_e^{21} = \cos^2 \frac{\pi f}{2f_0} - \frac{Z_1}{Z_3} \sin^2 \frac{\pi f}{2f_0}, \quad (2a)$$

$$D_e^{21} = \cos^2 \frac{\pi f}{2f_0} - \frac{Z_3}{Z_1} \sin^2 \frac{\pi f}{2f_0}$$

$$C_e^{21} = j \frac{(Z_3 + Z_1)}{2} \sin \frac{\pi f}{f_0}, \quad B_e^{21} = \frac{j}{2} \left( \frac{1}{Z_1} + \frac{1}{Z_3} \right) \sin \frac{\pi f}{f_0}. \quad (2b)$$

Similarly, even-mode  $S$ -parameters between ports 3 and 1 can be derived from the modified-even equivalent circuit as shown in Fig. 2b and expressed as follows:

$$S_{11e}^{31} = \frac{A_e^{31}k_1^2Z_c + B_e^{31}k_1^2 - C_e^{31}(1+k_1^2)Z_aZ_c - D_e^{31}(1+k_1^2)Z_a}{A_e^{31}k_1^2Z_c + B_e^{31}k_1^2 + C_e^{31}(1+k_1^2)Z_aZ_c + D_e^{31}(1+k_1^2)Z_a} \quad (3a)$$

$$S_{31e}^{31} = \frac{2\sqrt{(1+k_1^2)Z_aZ_c}}{A_e^{31}k_1^2Z_c + B_e^{31}k_1^2 + C_e^{31}(1+k_1^2)Z_aZ_c + D_e^{31}(1+k_1^2)Z_a} \quad (3b)$$

where

$$x_1 = \frac{\left( \sqrt{(2/Z_cZ_0)}a_1b_1 - (2a_4/Z_cZ_0) - (a_3b_1b_2/Z_a)\sqrt{(2/Z_0Z_c)} - (a_1b_2/Z_a) \right) + j\left\{ \sqrt{(2/Z_cZ_0)}a_2b_1 + (2a_5/Z_cZ_0) + (a_3b_1b_2/Z_a)\sqrt{(2/Z_0Z_c)} - (a_2b_2/Z_a) \right\}}{\sqrt{(2/Z_cZ_0)}a_3b_1 - a_2 + j\{a_4b_1\sqrt{(2/Z_cZ_0)} + a_1\}} \quad (4e)$$

$$x_2 = \frac{\left( \sqrt{(2/Z_cZ_0)}a_5b_1 - (2a_4/Z_cZ_0) + (a_3b_1b_2/Z_a)\sqrt{(2/Z_0Z_c)} + (a_3b_2/Z_a) \right) - j\left\{ \sqrt{(2/Z_cZ_0)}a_6b_1 - (2a_5/Z_cZ_0) + (a_3b_1b_2/Z_a)\sqrt{(2/Z_0Z_c)} + (a_6b_2/Z_a) \right\}}{\sqrt{(2/Z_cZ_0)}a_3b_1 - a_2 + j\{a_4b_1\sqrt{(2/Z_cZ_0)} + a_1\}} \quad (4f)$$

$$A_e^{31} = \frac{x_2 + x_1}{x_2 - x_1} \cos \frac{\pi f}{2f_0} + j \frac{2x_1x_2Z_2}{x_2 - x_1} \sin \frac{\pi f}{2f_0} \quad (4a)$$

$$B_e^{31} = \frac{2}{x_2 - x_1} \cos \frac{\pi f}{2f_0} + j \frac{x_2 + x_1}{x_2 - x_1} Z_2 \sin \frac{\pi f}{2f_0} \quad (4b)$$

$$C_e^{31} = \frac{2x_1x_2}{x_2 - x_1} \cos \frac{\pi f}{2f_0} + j \frac{x_2 + x_1}{x_2 - x_1} \frac{1}{Z_2} \sin \frac{\pi f}{2f_0} \quad (4c)$$

$$D_e^{31} = \frac{x_2 + x_1}{x_2 - x_1} \cos \frac{\pi f}{2f_0} + j \frac{1}{Z_2} \sin \frac{\pi f}{2f_0} \quad (4d)$$

(see (4e))  
(see (4f))

$$a_1 = b_1^2 - C_{\text{eff}}^2 \csc^2 \frac{\pi f}{2f_0} - \frac{Z_{\text{CL}} C_{\text{eff}} b_1 b_2}{Z_0} \quad (4g)$$

$$a_2 = \frac{Rb_2}{Z_0} \left( b_1^2 - C_{\text{eff}}^2 \csc^2 \frac{\pi f}{2f_0} \right) \quad (4h)$$

$$a_3 = R \left( b_1^2 - C_{\text{eff}}^2 \csc^2 \frac{\pi f}{2f_0} \right), \quad a_4 = Z_{\text{CL}} C_{\text{eff}} b_1 \quad (4i)$$

$$a_5 = \frac{Z_{\text{CL}} C_{\text{eff}} b_1 b_3}{Z_0} - C_{\text{eff}}^2 \csc^2 \frac{\pi f}{2f_0} + b_1^2 \quad (4j)$$

$$a_6 = \frac{Rb_3}{Z_0} \left( b_1^2 - C_{\text{eff}}^2 \csc^2 \frac{\pi f}{2f_0} \right) \quad (4k)$$

$$b_1 = \cot \frac{\pi f}{2f_0}, \quad b_2 = \tan \frac{\pi f}{4f_0}, \quad b_3 = \cot \frac{\pi f}{4f_0} \quad (4l)$$

$$Z_{\text{CL}} = \frac{2Z_{0e}Z_{0o}}{Z_{0e} - Z_{0o}}. \quad (4m)$$

$$C_{\text{eff}} = \frac{Z_{0e} - Z_{0o}}{Z_{0e} + Z_{0o}} \quad (4n)$$

where  $Z_{\text{CL}}$ ,  $Z_{0e}$ ,  $Z_{0o}$ ,  $C_{\text{eff}}$ , and  $k_1^2$  are the characteristic impedance, even-mode impedance, and odd-mode impedance, and coupling coefficient of the coupled lines and power-division ratio of WPD, respectively.

The modified odd-mode equivalent circuit of proposed arbitrary terminated unequal PD is shown in Fig. 3. Since no power transferred during odd-mode excitation, output reflection coefficients can be derived as follows:

(see (5))

$$S_{33} = \frac{2Z_c((1/Z_c^2) - x_1x_2) + j((Z_cx_2b_1/Z_2) + (Z_cx_1b_1/Z_2) - (2b_1/Z_2))}{(x_1 + x_2)(2 - j(Z_c b_1/Z_2)) + ((2/Z_c) - j(2b_1/Z_2)) + 2Z_cx_1x_2} \quad (6)$$

For all matched ports at  $f=f_0$ , the values of reflection coefficients are set to zero ( $S_{ii}=0$ ). Under these conditions, the characteristic impedances of transmission lines are found as follows:

$$Z_1 = \sqrt{Z_a Z_c (1 + k_1^2)} k_1^2 \quad (7a)$$

$$Z_2 = \sqrt{Z_a Z_c \left( \frac{1 + k_1^2}{k_1^2} \right)} \quad (7b)$$

$$Z_3 = \sqrt{Z_b Z_c k_1^2} \quad (7c)$$

Furthermore, overall transmission  $S$ -parameters of the proposed arbitrary terminated unequal PD are determined as (8a and 8b) as no power transmission occurs during odd-mode excitation:

$$S_{21} = \frac{S_e^{21}}{\sqrt{1 + k_1^2}} \quad (8a)$$

$$S_{31} = \frac{k_1 S_e^{31}}{\sqrt{1 + k_1^2}} \quad (8b)$$

The GD associated with a different transmission path can be determined by the following relationship:

$$\tau_{21} = -\frac{1}{2\pi} \frac{d\angle S_{21}}{df} \quad (9a)$$

$$\tau_{31} = -\frac{1}{2\pi} \frac{d\angle S_{31}}{df} \quad (9b)$$

Finally, the transmission  $S$ -parameter magnitudes and GDs associated with the different transmission paths of the proposed PD at  $f_0$  can be simplified as follows:

$$|S_{21}|_{f=f_0} = \frac{1}{\sqrt{1 + k_1^2}} \quad (10a)$$

$$|S_{31}|_{f=f_0} = \frac{k_1}{\sqrt{1 + k_1^2}} \left| \frac{Z_0 - R}{Z_0 + R} \right| = \frac{k_1 k_2}{\sqrt{1 + k_1^2}} \quad (10b)$$

$$\tau_{21}|_{f=f_0} = \frac{\sqrt{(1 + k_1^2) Z_a (k_1^2 Z_c + Z_b)} + \sqrt{Z_b (k_1^2 Z_c + Z_a k_1^2 + Z_a)}}{8 f_0 \sqrt{k_1^2 (1 + k_1^2) Z_a Z_b Z_c}} \quad (10c)$$

$$\tau_{31}|_{f=f_0} = -\frac{1}{2 f_0} \quad (10d)$$

$$\left\{ \begin{aligned} & \frac{\left\{ \begin{aligned} & R Z_0 (2\sqrt{Z_c Z_0} - \sqrt{2} Z_c) + \sqrt{2} R^2 (2Z_0 + Z_c) \\ & + \sqrt{Z_c Z_0} (3R + Z_0 + \sqrt{2 Z_c Z_0}) (R - Z_0) \end{aligned} \right\}}{2\sqrt{Z_c Z_0} (R^2 - Z_0^2)} \\ & + \frac{Z_0 Z_{CL}}{C_{eff} (R^2 - Z_0^2)} \\ & - \frac{1}{4\sqrt{Z_a Z_c}} \left( \sqrt{\frac{1 + k_1^2}{k_1^2}} Z_a + Z_c \sqrt{\frac{k_1^2}{1 + k_1^2}} \right) \end{aligned} \right. \quad (10d)$$

where

$$k_2 = \left| \frac{Z_0 - R}{Z_0 + R} \right| \quad (11)$$

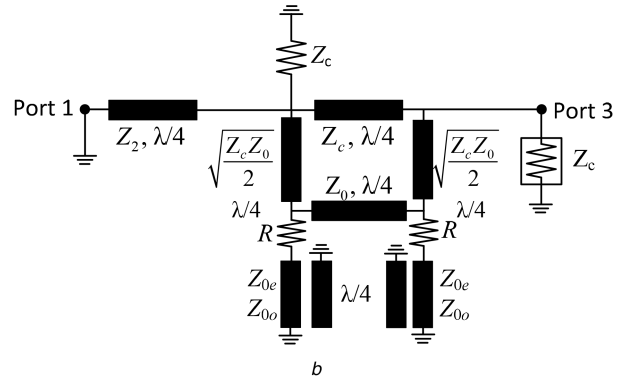
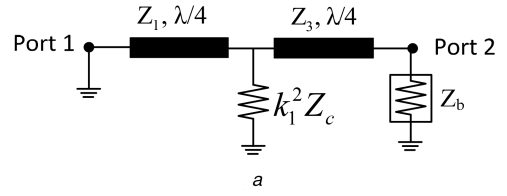


**Fig. 3** Modified odd-mode equivalent circuit of the proposed arbitrary terminated unequal power divider (a) Between ports 2 and 1 and, (b) Between ports 3 and 1

and  $Z_0 = 50 \Omega$ . Similarly, for the infinite isolation ( $S_{23} = 0$ ) between output ports, the value of the isolation resistor ( $R_{iso}$ ) can be found as follows:

$$R_{iso} = (1 + k_1^2) Z_c \quad (12)$$

As can be seen from (10a) and (10c), the transmission coefficient magnitude and GD associated with paths 2 and 1 depend only on  $k_1^2$ . Moreover, the GD between paths 2 and 1 can provide only PGD. However, the magnitude and GD between paths 3 and 1 depend on  $k_1$  and  $R$  as described by (10b) and (10d), respectively. Furthermore, the transmission path between ports 3 and 1 can provide NGD by properly choosing  $Z_{CL}$ ,  $C_{eff}$ , and  $R$ . NGD can be increased by either changing  $Z_{CL}$  or  $R$ . Moreover, the SA of paths 3 and 1 can be improved by choosing low  $C_{eff}$ , which can simplify fabrication.

For the illustrative understanding of the design equations of the arbitrary terminated unequal PD, the calculated characteristic impedance of lines  $Z_1$ ,  $Z_2$ ,  $Z_3$ , and transmission coefficients magnitudes are shown in Fig. 4 for different  $k_1^2$ . As can be seen from these figures, the proposed unequal PD can be designed with  $k_1^2 = 0.5$  to 2 without any fabrication difficulty. Moreover, the values of  $Z_1$  and  $Z_3$  are increased, while the value of  $Z_2$  is decreased with an increase of the power-dividing ratio.

Fig. 5 shows the calculated GD and transmission coefficient magnitude ( $|S_{31}|$  at  $f_0$ ) through ports 3 and 1 for different  $Z_{CL}$  and  $R$ . Meanwhile, the magnitudes of  $|S_{21}|$  and PGD through ports 2 and 1 remains constant for  $k_1^2 = 2$  and are not shown in these graphs. As clearly seen from Fig. 5a, NGD increases while the magnitude of  $|S_{31}|$  at  $f_0$  remains constant as  $Z_{CL}$  is increased. As shown in Fig. 5b, the NGD and magnitude of  $|S_{31}|$  at  $f_0$  increase towards a higher negative value when the value of  $R$  is decreased. A low value of  $R$  is preferable for a higher NGD; however, insertion loss through ports 3 and 1 increases, which require trade-off between insertion loss and NGD.

Fig. 6 shows the calculated response of the proposed unequal PD with different power-dividing ratios. As observed from the synthesised results shown in Fig. 6a, the magnitude of  $|S_{21}|$  is decreased and the magnitude of  $|S_{31}|$  is increased as  $k_1^2$  is changed

$$S_{22} = \frac{b_1((1/Z_3) + (1/Z_1) - (Z_b/k_1^2 Z_c Z_3)) + j((1/k_1^2 Z_c) - (Z_b/Z_3^2) + (Z_b/Z_1 Z_3) b_1^2)}{b_1((1/Z_3) + (1/Z_1) + (Z_b/k_1^2 Z_c Z_3)) + j((1/k_1^2 Z_c) + (Z_b/Z_3^2) - (Z_b/Z_1 Z_3) b_1^2)} \quad (5)$$

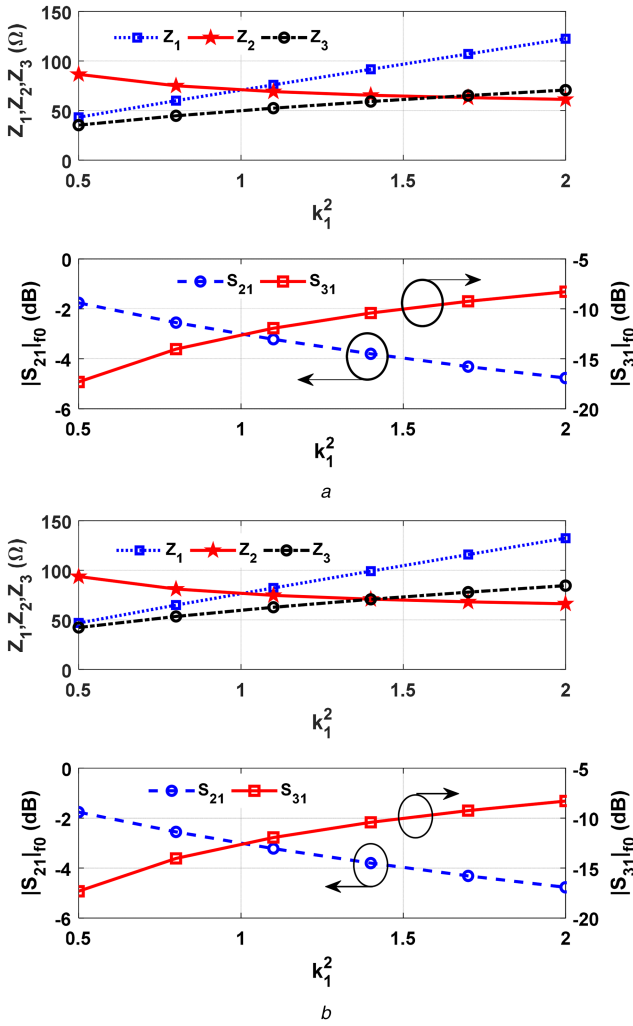


**Fig. 4** Calculated circuit parameters with  $Z_{CL} = 300 \Omega$ ,  $C_{eff} = -12.04 \text{ dB}$ ,  $R = 100 \Omega$  and different  $k_1^2$  for (a)  $Z_a = Z_b = Z_c = 50 \Omega$ , and (b)  $Z_a = 45 \Omega$ ,  $Z_b = 55 \Omega$ ,  $Z_c = 65 \Omega$

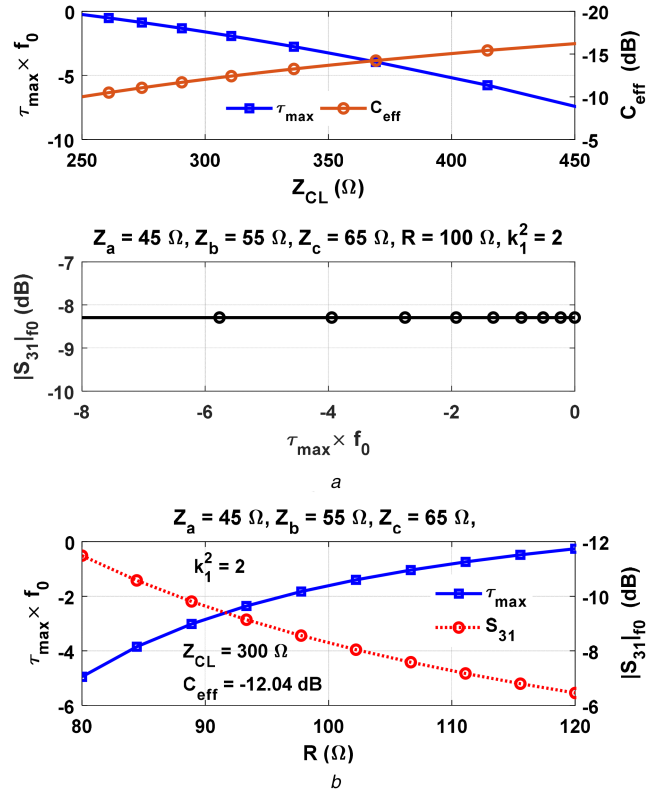
from 1 to 4. Moreover, the overall power-division ratio ( $|S_{31}/S_{21}|$ ) of the proposed circuit is also changed according to  $k_1^2$ . However, the GDs of the different transmission paths ( $\tau_{21}$  and  $\tau_{31}$ ) are almost constant for different  $k_1^2$  as shown in Fig. 4a and Table 1.

Fig. 6b shows the synthesised return losses ( $S_{ii}$ ) and isolation ( $S_{23}$ ) between output ports for different  $k_1^2$ . As shown in this figure, input/output ports are matched and the infinite isolation ( $S_{23}$ ) between output ports at  $f_0$  is obtained for all values of  $k_1$ . The phase difference between ports ( $|\angle S_{31} - \angle S_{21}|$ ) is  $180^\circ$  at  $f_0$  for the arbitrary  $k_1^2$ .

### 3 Simulation and measurement results

The design method of the proposed arbitrary terminated unequal PD is summarised as follows.

- Specify centre frequency  $f_0$ , power-division ratio of WPD  $k_1^2$ , maximum achievable NGD, SA, termination impedances  $Z_a$ ,  $Z_b$ , and  $Z_c$ .
- Calculate  $Z_1$ ,  $Z_2$ ,  $Z_3$ , and  $R_{iso}$  using (7a–7c) and (12) for specified  $k_1^2$ ,  $Z_a$ ,  $Z_b$ , and  $Z_c$ .
- Obtain the value of  $R$  for the specified SA using (10b).
- After obtaining the value of  $R$ , calculate NGD at  $f_0$  using (10d) by providing the value of  $Z_{CL}$  and  $C_{eff}$ .
- Compare the calculated achievable NGD ( $\tau_{cal}$ ) with the specified value ( $\tau_{req}$ ). If  $|\tau_{cal} - \tau_{req}| \leq 0.001 \text{ ns}$ ,  $Z_{CL}$  and  $C_{eff}$  are the



**Fig. 5** Calculated magnitude and group delay through ports 3 and 1 with different (a)  $Z_{CL}$  and, (b)  $R$

required values for the specified NGD. If this condition is not satisfied, then change  $Z_{CL}$ ,  $C_{eff}$ , and repeat the processes (d) and (e).

(f) Calculate  $Z_{0e}$  and  $Z_{0o}$  using (4m) and (4n).

(g) After getting final values of circuit parameters, obtain the width, length, and spacing of the coupled line and other transmission lines according to the substrate information and optimise the physical dimensions using a 3-D electromagnetic simulator.

For experimental demonstration purposes, the unequal PDs were fabricated at  $f_0$  of 2.14 GHz on the RT/Duroid 5880 substrate with a dielectric constant ( $\epsilon_r$ ) of 2.2 and thickness ( $h$ ) of 0.787 mm. The physical dimensions of fabricated circuits were optimised using ANSYS HFSS 15.

The goal of the design example I was to achieve NGD of  $-1 \text{ ns}$  and  $k_1^2 = 2$  under the assumption of the termination port reference impedance  $Z_a = Z_b = Z_c = 50 \Omega$  for measurement simplicity with a network analyser. Therefore, the calculated circuit parameters were given as  $Z_1 = 122.47 \Omega$ ,  $Z_2 = 61.24 \Omega$ ,  $Z_3 = 70.71 \Omega$ ,  $R_{iso} = 150 \Omega$ ,  $Z_{CL} = 346.66 \Omega$ ,  $C_{eff} = -12.74 \text{ dB}$ ,  $Z_{0e} = 104 \Omega$ ,  $Z_{0o} = 65 \Omega$ , and  $R = 100 \Omega$ . The physical dimensions of PD are shown in Fig. 7a after optimisation. Similarly, Fig. 7b shows a photograph of the fabricated PD.

Fig. 8a shows the simulated and measured magnitudes and GDs through different transmission paths of unequal PD. The measured  $|S_{21}|$  and  $|S_{31}|$  are  $-5.18$  and  $-10.93 \text{ dB}$ , respectively, at  $f_0 = 2.14 \text{ GHz}$ . Similarly, the measured GDs between different transmission paths are determined as  $\tau_{21} = 0.246 \text{ ns}$  and  $\tau_{31} = -1.143 \text{ ns}$  at  $f_0$ . The simulated and measured return losses and isolation are shown in Fig. 8b. The measured return losses are determined as  $|S_{11}| = -23.83 \text{ dB}$ ,  $|S_{22}| = -24.49 \text{ dB}$ , and  $|S_{33}| = -31.77 \text{ dB}$  at  $f_0$ . The isolation ( $|S_{32}|$ ) is higher than  $34.58 \text{ dB}$  in the overall bandwidth.

As shown in the previous results of the single coupled-line PD, the magnitude flatness and NGD bandwidth are small and are thus not practically applicable for commercial RF systems. Therefore, it is necessary to enhance the NGD bandwidth. One way

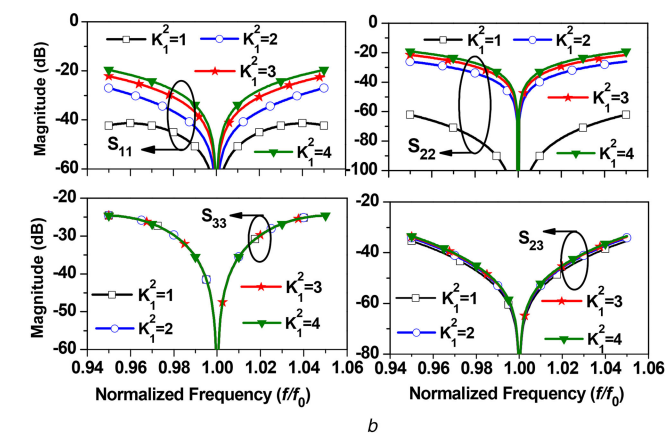
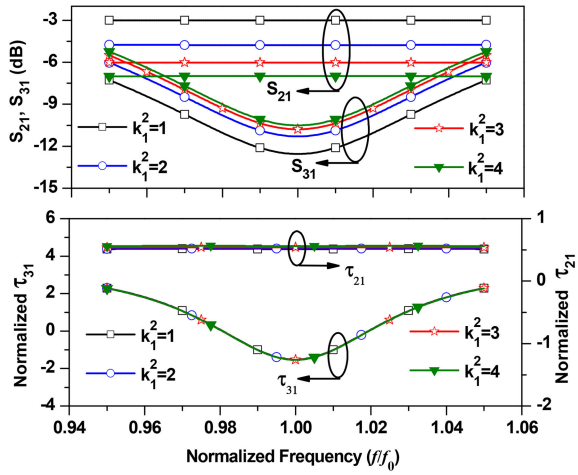


**Fig. 6** Synthesised results of unequal power divider with  $Z_a = Z_b = Z_c = 50 \Omega$  and different  $k_1^2$   
(a) Magnitude/group delay and (b) Return loss/isolation characteristics

**Table 1** Calculated circuit parameters of the proposed power divider with  $Z_a = Z_b = Z_c = 50 \Omega$ ,  $C_{\text{eff}} = -12.04 \text{ dB}$ ,  $Z_{\text{CL}} = 300 \Omega$ ,  $Z_{0e} = 100 \Omega$ ,  $Z_{0o} = 60 \Omega$ , and  $R = 100 \Omega$

$k_1^2$	Unit, $\Omega$				$S_{31}/S_{21}$ , dB	Group delay	
	$Z_1$	$Z_2$	$Z_3$	$R_{\text{iso}}$		$\tau_{21} \times f_0$	$\tau_{31} \times f_0$
1	70.7	70.7	50	100	9.54	0.51	-1.52
2	122.4	61.6	70.7	150	6.53	0.52	-1.53
3	173.2	57.7	86.6	200	4.77	0.52	-1.53
4	223.6	55.9	100	250	3.52	0.52	-1.53

to increase the NGD bandwidth and magnitude flatness is to connect two units of short-circuited coupled lines at different centre frequencies in parallel. For this purpose, the design example II with NGD of  $-1.4 \pm 0.5 \text{ ns}$ ,  $k_1^2 = 2$ , and  $Z_a = Z_b = Z_c = 50 \Omega$  was designed and fabricated. The circuit layout and photograph of the fabricated circuit are shown in Fig. 9. The calculated circuit parameters of the designed circuit are given as  $Z_1 = 122.47 \Omega$ ,  $Z_2 = 61.24 \Omega$ ,  $Z_3 = 70.71 \Omega$ ,  $R_{\text{iso}} = 150 \Omega$ . Similarly, the parameter coupled-line section of the NGD bandwidth enhanced PD shown in Fig. 9 are summarised as  $Z_{0e1} = Z_{0e2} = 100 \Omega$ ,  $Z_{0o1} = Z_{0o2} = 74 \Omega$ ,  $C_{\text{eff}1} = C_{\text{eff}2} = -16.51 \text{ dB}$ , and  $R = 125 \Omega$ . The centre frequency of the first and second coupled lines are assigned as  $f_{01} = 2.112 \text{ GHz}$ , and  $f_{02} = 2.17 \text{ GHz}$ .

The simulated and measured GDs and magnitudes of different transmission paths for prototype I (single coupled line) and prototype II (parallel connected coupled lines) are shown in Fig. 10a for comparison. From the experimental results, the magnitudes of  $|S_{21}|$  and  $|S_{31}|$  are  $-5.04$  and  $-13.09 \text{ dB}$ , respectively. Similarly, the measured GDs between different transmission paths are  $\tau_{21} = 0.226 \text{ ns}$  and  $\tau_{31} = -1.407 \pm 0.505 \text{ ns}$  at  $f_0 = 2.14 \text{ GHz}$ . As

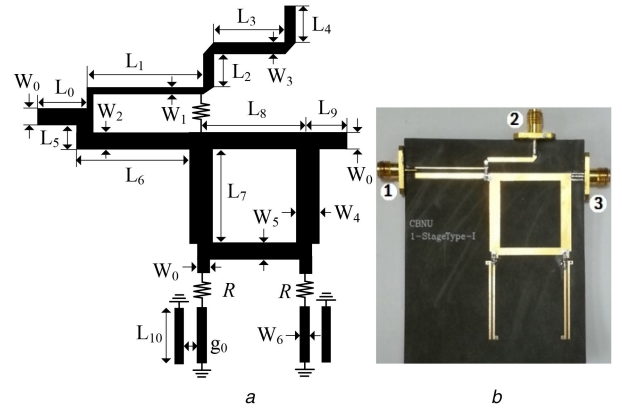


**Fig. 7** Unequal power divider

(a) EM-simulation layout and, (b) Fabricated circuit. Physical dimensions:  $L_0 = 4$ ,  $L_1 = 26$ ,  $L_2 = 2$ ,  $L_3 = 17$ ,  $L_4 = 6$ ,  $L_5 = 1.35$ ,  $L_6 = 26$ ,  $L_7 = 22.6$ ,  $L_8 = 23.1$ ,  $L_9 = 8.9$ ,  $L_{10} = 26.2$ ,  $W_0 = 2.4$ ,  $W_1 = 0.4$ ,  $W_2 = 1.72$ ,  $W_3 = 1.40$ ,  $W_4 = 3.90$ ,  $W_5 = 2.4$ ,  $W_6 = 0.8$ ,  $g_0 = 0.6$  (Unit: mm)

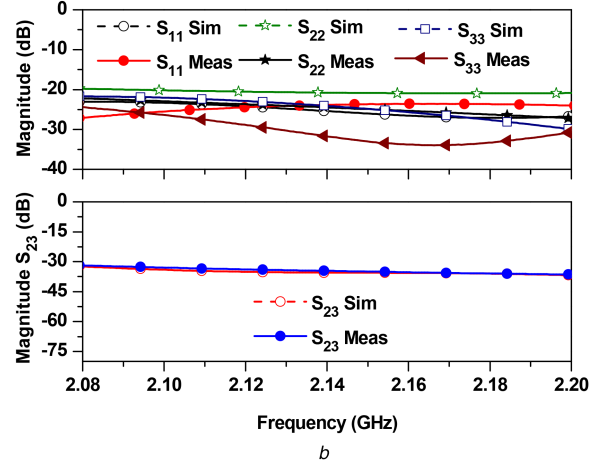
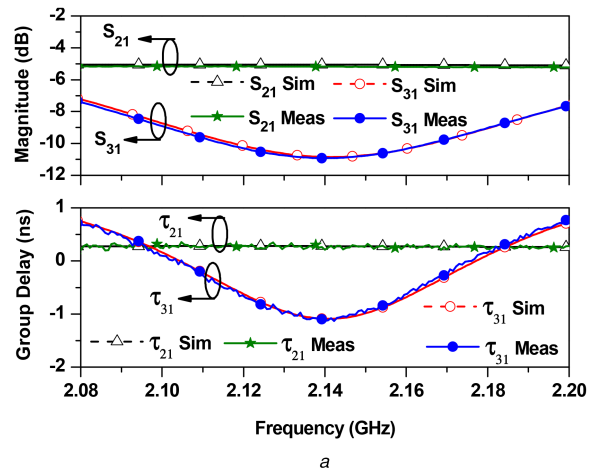


**Fig. 8** Simulated and measured results of the proposed unequal power divider

(a) Magnitude/group delay and (b) Return losses/isolation characteristics

clear from these results, the NGD bandwidth (bandwidth of  $\text{GD} < 0$ ) as well as the magnitude flatness of prototype II are wider than prototype I. Similarly, the simulated and measured return losses and isolation are shown in Fig. 10b. The performance comparison of the proposed circuit with the state of art is shown in Table 2. As observed from the table, the proposed PD provides arbitrary termination port impedances as well as power-division ratios.

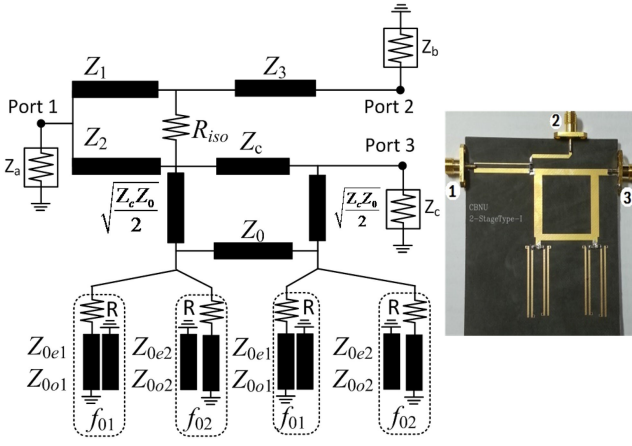


Fig. 9 Structure and photograph of fabricated parallel connected coupled lines for NGD bandwidth enhancement

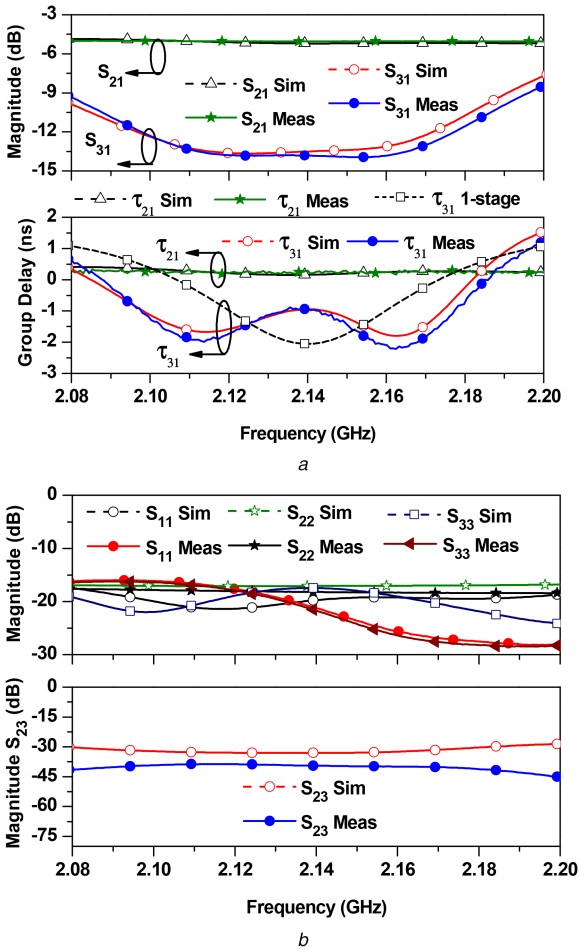


Fig. 10 Simulated and measured results of unequal power divider with parallel connected coupled lines (a) Magnitude/group delay and (b) Return loss/isolation characteristics

#### 4 Conclusion

In this paper, we investigated the GD characteristics of an arbitrary power-division ratio PD combined with an NGD circuit using generalised design equations. From the analytical analysis of this circuit, it is found that the magnitude and GD of the PGD path depend only on the power-division ratio, whereas the magnitude and GD of the NGD path depend on the power-division ratio as well as the on NGD circuit. NGD can be controlled by even- and odd-mode impedances as well as a series-connected resistor of short-circuited coupled lines. For experimental validation, unequal PD is designed, fabricated, and measured. Measurement results have a good agreement with simulations as well as the theoretical

Table 2 Performance comparison with the state of the arts

$f_0$ , GHz	Unit, dB		Group delay, ns		Unit, MHz	B	C
	$S_{21}$	$S_{31}$	$A$	$\tau_{21} f_0$			
[5]	2	-0.21 -13.21	yes	0.195	0.172	x	no no
[6]	1	-0.46 -10	yes	0.543	0.606	x	yes no
[7]	1	-0.41 -10.41	yes	0.611	0.601	x	no no
[8]	1	-0.46 -9.99	yes	0.325	0.325	x	no no
[18]	2.14	-9.29 -9.30	no	-1.161	-1.170	80	no no
[19]	2.14	-5.98 -5.98	yes	-0.861	-0.86	80	no no
[20]	2.14	-2.96 -24.35	yes	0.341	-0.529	100	no yes
[21]	2.14	-4.98 -7.48	yes	0.341	-0.852	60	no yes
[22]	2.14	-6.95 -6.97	no	-0.542	-0.542	60	no no
this work <sup>I</sup>	2.14	-5.18 -10.93	yes	0.246	-1.143	80	yes yes
this work <sup>II</sup>	2.14	-5.04 -13.09	yes	0.226	$-1.407 \pm 0.5$	110	yes yes

A: Arbitrary power-division ratio ( $k^2$ ).

B: Arbitrary port impedances ( $R_a, R_b, R_c$ ).

C: Negative and positive group delay through different transmission paths.

NGD BW: Negative group delay bandwidth when group delay <0.

predicted values. For NGD bandwidth and magnitude flatness enhancement, parallel connected coupled lines with slightly different frequencies in the PD were designed and fabricated. The proposed circuit can be employed as a feed network of series-fed antenna arrays to minimise the beam-squint problem.

#### 5 Acknowledgments

This research was supported by the Basic Science Research Program through the National Research Foundation of Korea (NRF) funded by the Ministry of Education, Science and Technology (2016R1D1A1A09918818) and in part by Korean Research Fellowship Program through the National Research Foundation of Korea (NRF) funded by ministry of Science and ICT (2016H1D3A1938065).

#### 6 References

- [1] Wilkinson, E.J.: 'An N-way hybrid power divider', *IEEE Trans. Microw. Theory Tech.*, 1960, **8**, (1), pp. 116–118
- [2] Ahn, H.R., Wolff, I.: 'General design equations, small-sized impedance transformers, and their applications to small-sized impedance transformers', *IEEE Trans. Microw. Theory Tech.*, 2001, **49**, (7), pp. 1277–1288
- [3] Wan, K.L., Chow, Y.L., Luk, K.M.: 'Simple design of dual-frequency unequal power-divider', *IET Electron. Lett.*, 2001, **37**, (19), pp. 1171–1173
- [4] Cheng, K.M., Li, P.: 'A novel power-divider design with unequal power dividing ratio and simple layout', *IEEE Trans. Microw. Theory Tech.*, 2009, **57**, (6), pp. 1589–1594
- [5] Ahn, H.R., Nam, S.: 'Wideband microstrip coupled-line ring hybrids for high power division ratios', *IEEE Trans. Microw. Theory Tech.*, 2013, **61**, (5), pp. 1768–1780
- [6] Ahn, H.R.: 'Compact CVT/CCT-unequal power dividers for high-power division ratios and design methods for arbitrary phase differences', *IEEE Trans. Microw. Theory Tech.*, 2014, **62**, (12), pp. 2954–2964
- [7] Ahn, H.R., Kim, Y., Kim, B.: 'Planar 10:1 unequal three-port dividers using general design equations', *IET Electron. Lett.*, 2012, **48**, (15), pp. 934–935
- [8] Li, B., Wu, X., Wu, W.: 'A 10:1 unequal Wilkinson power divider using coupled lines with two shorts', *IEEE Microw. Wirel. Compon. Lett.*, 2009, **19**, (12), pp. 789–791
- [9] Mirzaei, H., Eleftheriades, G.V.: 'Realizing non-Foster reactive elements using negative group delay networks', *IEEE Trans. Microw. Theory Tech.*, 2013, **61**, (12), pp. 4322–4332
- [10] Choi, H., Jeong, Y., Kim, C.D., et al.: 'Efficiency enhancement of feedforward amplifiers by employing a negative group delay circuit', *IEEE Trans. Microw. Theory Tech.*, 2010, **58**, (5), pp. 1116–1125
- [11] Choi, H., Jeong, Y., Kim, C.D., et al.: 'Bandwidth enhancement of an analog feedback amplifier by employing a negative group delay circuit', *Prog. Electromagn. Res.*, 2010, **105**, pp. 253–272
- [12] Jeong, Y., Choi, H., Kim, C.D.: 'Experimental verification for time advancement of negative group delay in RF electronics circuits', *Electron. Lett.*, 2010, **46**, (4), pp. 306–307
- [13] Lucyszyn, S., Robertson, I.D., Aghvami, A.H.: 'Negative group delay synthesizer', *Electron. Lett.*, 1993, **29**, (9), pp. 798–800

- [14] Lucyszyn, S., Robertson, I.D.: 'Analog reflection topology building blocks for adaptive microwave signal processing applications', *IEEE Trans. Microw. Theory Tech.*, 1995, **43**, (3), pp. 601–611
- [15] Chaudhary, G., Jeong, Y., Lim, J.: 'Microstrip line negative group delay filters for microwave circuits', *IEEE Trans. Microw. Theory Tech.*, 2014, **62**, (2), pp. 234–243
- [16] Chaudhary, G., Jeong, Y.: 'Low signal attenuation negative group delay network topologies using coupled lines', *IEEE Trans. Microw. Theory Tech.*, 2014, **62**, (10), pp. 2316–2324
- [17] Mirzaei, H., Eleftheriades, G.V.: 'Arbitrary-angle squint-free beam forming in series-fed antenna arrays using non-Foster elements synthesized by negative group delay networks', *IEEE Trans. Antenna Propag.*, 2015, **63**, (5), pp. 1997–2010
- [18] Chaudhary, G., Jeong, Y.: 'A design of power divider with negative group delay characteristics', *IEEE Microw. Wirel. Compon. Lett.*, 2015, **25**, (6), pp. 394–396
- [19] Chaudhary, G., Jeong, Y.: 'Arbitrary power division ratio rat-race coupler with negative group delay characteristics', *IEEE Microw. Wirel. Compon. Lett.*, 2016, **26**, (8), pp. 565–567
- [20] Chaudhary, G., Park, J., Wang, Q., *et al.*: 'A design of unequal power divider with positive and negative group delays'. Proc. European Microwave Conf., Paris, France, 2015
- [21] Chaudhary, G., Jeong, Y.: 'Negative group delay phenomenon analysis in power divider: Coupling matrix approach', *IEEE Trans. Compon. Packag. Manuf. Technol.*, 2017, **7**, (9), pp. 1543–1551
- [22] Chaudhary, G., Jeong, Y.: 'A finite unloaded quality-factor resonators based negative group delay circuit and its application to design power divider', *Microw. Opt. Technol. Lett.*, 2016, **58**, (12), pp. 2918–2921
- [23] Wu, Y., Wang, H., Zhuang, Z., *et al.*: 'A novel arbitrary terminated unequal coupler with bandwidth-enhanced positive and negative group delay characteristics', *IEEE Trans. Microw. Theory Tech.*, 2018, **66**, (5), pp. 2170–2184
- [24] Ahn, H.R.: 'Asymmetric passive components in microwave integrated circuits' (Wiley & Sons Inc., Hoboken, NJ, USA, 2006)